

# Asymmetric ( $e,2e$ ) study of the 100-eV ionization of the $1\pi_g$ , $1\pi_u$ , and $3\sigma_g$ molecular orbitals of $O_2$

J. Yang and J. P. Doering

*Department of Chemistry, Johns Hopkins University, Baltimore, Maryland 21218*

(Received 18 August 2000; published 14 February 2001)

The relative triple differential cross section for 100-eV electron-impact ionization of the three outer molecular orbitals of  $O_2$  has been studied in an asymmetric ( $e,2e$ ) experiment. The angular distribution of low-energy ejected electrons was measured from  $30^\circ$  to  $125^\circ$  with respect to the incident beam direction for an incident electron scattering angle of  $4^\circ$  and ejected-electron energies of 3.5, 6.0, and 11.0 eV. The ionization of the outer  $1\pi_g$  orbital that leads to the formation of an  $O_2^+$  ion in the  $X^2\Pi_g$  state was observed to be accompanied by the ejection of a low energy electron  $90^\circ$  to the incident beam direction on the binary side. Binary results for the other two orbitals,  $1\pi_u$  and  $3\sigma_g$ , to give the  $a^4\Pi_u$  and  $b^4\Sigma_g^+$  states were similar to previous results for the analogous orbitals in  $N_2$  with ejection directions of  $75^\circ$  and  $45^\circ$  to the incident beam direction, respectively. In contrast to the  $N_2$  results, the recoil peak for all cases was found to be aligned approximately  $180^\circ$  to the momentum transfer direction. Possible mechanisms for the binary low-energy electron ejection at angles so far removed from the momentum transfer direction are discussed.

DOI: 10.1103/PhysRevA.63.032717

PACS number(s): 33.80.-b

## INTRODUCTION

Coincidence ionization, or ( $e,2e$ ), experiments in which the two outgoing electrons have very unequal energies are of interest for several reasons. The cross section for ionization is largest for the ionization events in which the sharing of energy between the two outgoing electrons is most unequal or asymmetric [1,2]. Since these events are the most probable ionization processes, study of the ( $e,2e$ ) cross sections in this regime allows the partial cross sections or branching ratios to various final states of the residual ion to be investigated [3]. The angular distribution of low-energy ejected electrons that is given by the triple differential cross section (TDCS) is also of interest in the study of the interactions that lead to ionization of the neutral target.

Compared to atoms, very little work has been done so far on the asymmetric ( $e,2e$ ) TDCS for molecules. Our work on molecular nitrogen and oxygen has been described in four previous papers [4–7]. Two of the papers [4,5] reported partial branching ratios for production of various final states of  $N_2^+$  and  $O_2^+$  by 100-eV electron impact on the neutral molecules. The third [6] reported the distribution among vibrational states of the  $N_2^+$  ions produced in the ground and first-excited electronic states by 100-eV electron impact ionization of  $N_2$ . The fourth [7] reported the angular distributions of low-energy ejected or secondary electrons that accompany ionization of the two outermost molecular orbitals of  $N_2$ . In the present paper, we report the corresponding angular distributions of the low-energy ejected electrons that result from ionization of the three lowest ionization potential molecular orbitals of  $O_2$  to produce three electronic states of the  $O_2^+$  ion.

100-eV electron impact ionization of molecules usually produces a significant fraction of the residual ions in excited electronic states. The cross section for producing each final state is triply differential if the usual convention of considering only in-plane scattering is followed [7,8]. The three

independent variables are usually taken to be  $\theta'_0$ , the angle through which the incident electron is scattered,  $\theta_{ej}$ , the ejection angle of the low-energy ejected or secondary electron, and  $E_{ej}$  the energy of the ejected electron. These variables and the conventional ‘‘Ehrhardt’’ polar plot [2] used for display of the TDCS are all shown schematically in Fig. 1. The three variables do not define the final state of the residual ion. The final state of the ion is determined from the measurement of the energy loss of the incident electron. A separate TDCS must be reported for each final state.

The most interesting variable is  $\theta_{ej}$  since the ejected electrons are distributed over a wide angular range. In atoms, the ejected electrons are found in two lobes centered along and opposite to the momentum transfer direction [2] as predicted by first-order theory. These are known as the ‘‘binary’’ and ‘‘recoil’’ lobes of the TDCS [1]. The recoil lobe is often larger than the binary lobe [7] and there are deviations of the centers of the lobes from the momentum transfer direction.

As discussed previously [7], the angular resolution of the apparatus as set up for these measurements was  $4^\circ$ . The  $4^\circ$  angular bandpass centered on  $4^\circ$  scattering angle gives a good sampling of the interesting range of  $\theta'_0$ . Increasing  $\theta'_0$  further leads to a very rapid decrease in signal.

In our previous work [7], ionization of the  $3\sigma_g$  and  $1\pi_u$  outer molecular orbitals of  $N_2$  was observed. Although these two orbitals are only 1.11 eV apart in energy, the angular distributions of the ejected electrons that accompanied their ionization were quite different. For the  $3\sigma_g$  orbital, electron ejection in the binary direction was centered around  $-50^\circ$  while that for the  $1\pi_u$  was near  $-80^\circ$ , very far from the momentum transfer direction near  $-30^\circ$ . The recoil electron distribution was typically shifted to a smaller angle than the ‘‘recoil direction’’ (defined for the purposes of this discussion as  $180^\circ$  from the momentum transfer direction). This is opposite to what is generally observed in atomic ionization [2].

Comparison of data from  $N_2$  and  $O_2$  is useful since  $O_2$  has

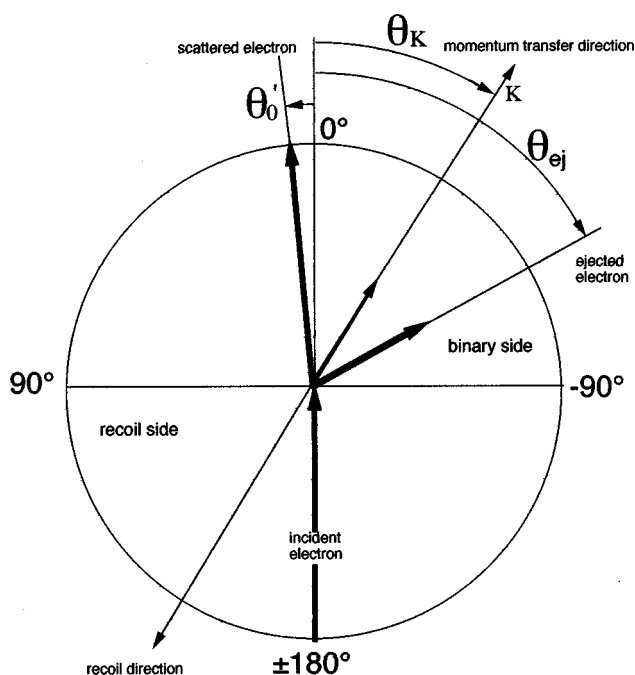


FIG. 1. Schematic diagram of coordinates used to display the triple differential cross section for ionization leading to a specific final electronic state of the residual ion. The angular distribution of ejected electrons is plotted vs ejection angle at constant scattered-electron angle and ejected-electron energy [2]. The incident electron enters from the bottom at  $\pm 180^\circ$  and is scattered to the left. The ejected-electron direction and momentum-transfer direction are shown for the case of an electron ejected in the binary direction.

the same two molecular orbitals as  $N_2$  ( $3\sigma_g$  and  $1\pi_u$ ), but reversed in energy [9], with an additional outer  $1\pi_g$  orbital containing two unpaired electrons. 100-eV asymmetric ( $e,2e$ ) experiments are generally sensitive to the interactions between the incident electron and the target [2] so it appeared possible to compare the ionization of analogous molecular orbitals in different environments by comparing the results from  $O_2$  and  $N_2$ . We also anticipated that ionization of the two unpaired electrons of the outer molecular orbital of  $O_2$  would produce unusual effects, very different from ionization of paired electrons.

## EXPERIMENT

A detailed description of the apparatus has already been published [7]. Details relating to the experiments on  $O_2$  can be found in the paper describing the  $O_2$  branching ratio results [5].

Briefly, the apparatus consists of an electron monochromator, a scattered primary electron analyzer, and a low-energy ejected electron analyzer. All three electron spectrometers use hemispherical electrostatic deflectors. The beam of electrons produced by the monochromator was crossed with an  $O_2$  gas jet from a hypodermic needle source. The scattered primary and ejected secondary electrons were energy-analyzed at variable angles with respect to the incident beam direction. The electrons were detected by electron multipliers and conventional amplifier and discriminator cir-

cuits that passed the digital pulses to the coincidence electronics. The entire apparatus was housed in a large, magnetically shielded, stainless-steel bell jar approximately 0.5 m in diameter and 1.0 m high.

A double shield of high-permeability material was used to reduce the ambient magnetic field to a negligible value [7] inside the bell jar. The shields were fabricated so that one fits inside the bell jar and one fits outside. Like the bell jar, they had open lower ends. The electron spectrometers were supported inside the bell jar one diameter away from the open bottom by the baffle used for differential pumping of the source. Measurements of the residual magnetic field at the position of the spectrometers showed that the ambient geomagnetic field of approximately 0.6 G was reduced to  $<5$  mG.

The method used for computerized data collection and analysis has also been described in detail [6]. For each final state of the ion, there is a characteristic energy equal to the energy of the ejected electron plus the ionization potential of the molecular orbital from which the electron is removed. When the energy loss of the incident electron is equal to this value, an increase in the coincidence rate appears in the coincidence rate vs energy loss spectrum. At other values of the energy loss, the background, uncorrelated accidental coincidence rate is observed.

Each pulse received from the coincidence electronics had associated with it a time parameter and an energy loss parameter. The memory of the computer was configured so that there was a time spectrum for each value of energy loss. The magnitude of the coincidence peak in each time spectrum was plotted as a function of energy loss. This coincidence energy loss spectrum is one final form of the data. Examples of coincidence energy loss spectra of this type for  $O_2$  have been published previously [5].

In general, oxygen is more difficult to work with than  $N_2$ . This is partly due to the greater chemical reactivity of  $O_2$  that causes the hot filament electron source to burn out more rapidly. It is also a result of the fact that the total ionization intensity in  $O_2$  is distributed among seven final states of  $O_2^+$  while  $N_2^+$  has only three states. A survey coincidence energy loss spectrum of  $O_2$  taken with the apparatus, has been published previously [5].

Data were acquired in both a "spectrum" and an "ejected angle" mode [7]. In the spectrum mode, a time spectrum is recorded at each value of energy loss. This is similar to a separation spectrum except that in our apparatus, the ejected energy was kept constant while the energy loss was scanned at constant  $E_{ej}$  and  $\theta_{ej}$ . In the ejected angle mode, time spectra are recorded as a function of  $\theta_{ej}$  for a fixed separation energy corresponding to a particular final-ion state. The ejected angle data must be suitably normalized in order to determine the relative amplitudes of the signals from the different final-ion states. This was usually done by normalizing the data at each of the angles to a coincidence energy loss spectrum taken at one angle.

The intensity of the scattered signal is proportional to the mutual volume of the incident electron beam and the neutral beam as viewed by the scattered- and ejected-electron detectors. Since all the experiments were done at the same scat-

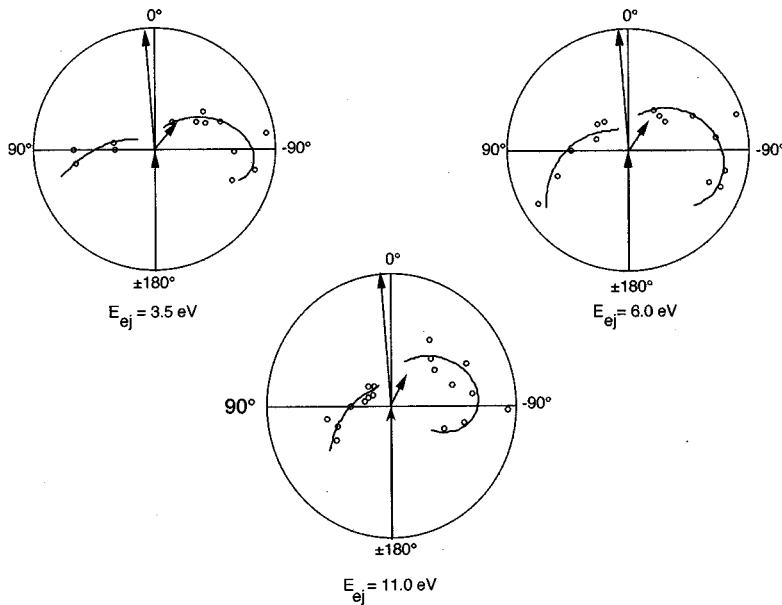


FIG. 2. Experimental results for relative  $O_2$  triple differential cross section vs  $\theta_{ej}$  for ionization of the  $1\pi_s$  orbital of  $O_2$  to give the  $X^2\Pi_g$  state of the residual  $O_2^+$  ion. The incident energy and scattered-electron angle were 100 eV and  $4^\circ$  in all cases. Results are shown for  $E_{ej}$  of 3.5, 6.0, and 11.0 eV. The direction of momentum transfer is shown by the small vector. The points are the experimental data. The solid lines are least squares fits to the experimental data and are intended to guide the eye.

tered electron angle ( $4^\circ$ ), it was only necessary to account for the changes in effective volume with ejected-electron angle. The dependence of the scattering volume on secondary electron ejection angle was determined by measuring the angular dependence of an autoionization process in  $O_2$ . We have previously reported the observation of an autoionization process in  $O_2$  [10] that produces an isotropic flux of electrons that can be observed in the coincidence energy loss spectrum for very small ejected-electron energies. The variation of the scattering signal due to the change in scattering volume with angle was determined by measuring the apparent variation in intensity of this isotropic electron flux as a function of scattering angle. The angular dependence was found to be well represented by the function  $(1 + \cos^2 \theta_{ej})$  [7]. In the present work, this normalization was used differently at 3.5 and 11 eV. For the 3.5-eV data, the autoionization peak appeared in the coincidence energy loss spectrum. The intensities of the various peaks at different angles were normalized to a constant value of the autoionization intensity. For the 11-eV data, the autoionization peak did not appear in the energy loss spectra so it was necessary to use a different method of normalization. The 11-eV data were collected using the ‘‘angular scan’’ method. This gave relative values of the cross section for one final state at different values of  $\theta_{ej}$ . The  $(1 + \cos^2 \theta_{ej})$  correction factor was applied to the intensities measured at different values of  $\theta_{ej}$ . In order to normalize the data for the different transitions at the different values of  $\theta_{ej}$  a complete energy loss spectrum was obtained at a single reference angle. The relative values of the true coincidence rates were then used to normalize the angular data to the data at the reference angle. This gave the corrected values of the intensities as a function of  $\theta_{ej}$ .

At 6 eV, the  $O_2$  autoionization process was not used for normalization since the 5 eV TDCS for argon was available, both from experiment [11] and theory [12]. A mixture of the two gases was admitted to the spectrometer and the  $O_2/Ar$  ratio was determined from an energy loss spectrum of the 100-eV incident electron flux scattered at  $4^\circ$  that contained

peaks corresponding to electronic transitions of known optical oscillator strengths in both species. Using the small-angle relationship between the generalized and optical oscillator strengths as described previously [13], it was possible to calculate the  $O_2/Ar$  ratio and from this and the known argon TDCS, the TDCS for  $O_2$  could be determined.

The measured energy of the ejected electrons contained a contact potential contribution. The true energy of the ejected electrons was obtained by measuring the apparent position in energy of the 19.3-eV He resonance as described previously [7].

## RESULTS

Results for ejected-electron energies of 3.5, 6.0, and 11.0 eV for the  $X^2\Pi_g$ ,  $a^4\Pi_u$  and  $b^4\Sigma_g^+$  states of  $O_2^+$  are shown in Figs. 2, 3, and 4. The direction of the momentum transfer vector is shown on each plot. Since our interest here is in the angular distributions of the ejected electrons, we have normalized the data to a single maximum value to facilitate comparison of the ejected-electron distributions. It should be remembered, however, that the triple differential cross section decreases rapidly with increasing ejected energy. Since this aspect of the differential cross section has been well investigated in double differential cross section experiments [1], we have not made any measurements of the TDCS as a function of ejected-electron energy.

Figure 2 shows the results for the  $X^2\Pi_g$  state. The distribution of ejected electrons accompanying ionization to the  $X^2\Pi_g$  state is the most unusual distribution observed for any of the  $O_2^+$  states. The maximum of the binary peak is aligned with the  $-90^\circ$  direction, far from the momentum transfer direction,  $-34^\circ$ . The results at the three ejected-electron energies are quite similar. Since the recoil-peak data from all the states appears to show the same effects, the recoil data will be discussed later.

Figures 3 and 4 show data for the  $a^4\Pi_u$  and  $b^4\Sigma_g^+$  states, respectively. The binary results are quite similar to

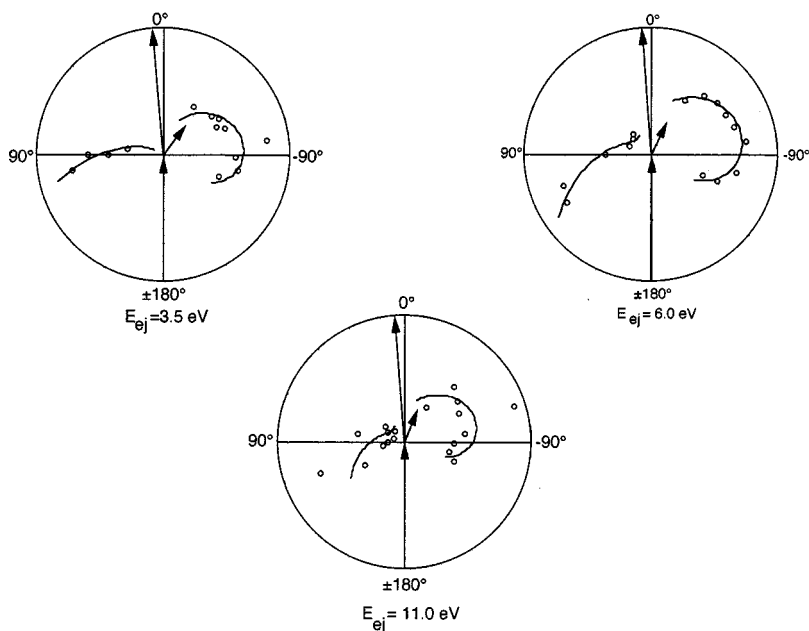


FIG. 3. Same as Fig. 2 except for ionization of the  $1\pi_s$  orbital of  $O_2$  to give the  $a^4\Pi_s$  state of the  $O_2^+$  ion.

those for the analogous orbital in  $N_2$ . The signal to noise ratio is not as good as for  $N_2$  because of the weaker signals for  $O_2$  as noted above. The binary peak for the  $a^4\Pi_u$  state appears to be centered near  $-75^\circ$  for all three ejected energies. For the  $b^4\Sigma_g^+$  state, the 3.5- and 6-eV binary maxima are near  $-45^\circ$ . At 11 eV, the signal to noise ratio was too poor to allow a distribution to be obtained for the  $b^4\Sigma_g^+$  state. The 3.5- and 6.0-eV binary results are very similar to those in  $N_2$ . Removal of an electron from the  $1\pi_g$  orbital of  $N_2$  gives a distribution with a peak near  $-75^\circ$ . For the  $3\sigma_g$  orbital, the peak is near  $-50^\circ$ .

The results for the recoil electrons are similar for all the  $O_2$  orbitals and can be most clearly seen in Fig. 3, which shows the 6-eV ejected-energy results. Unfortunately, only the edge of the recoil distribution is accessible with the present apparatus. The 6.0- and 11.0-eV distributions extend out to the  $125^\circ$  limit of the apparatus. The 11.0-eV cross section is smaller than the 6.0-eV cross section at this angle. This could be a result of a smaller overall cross section for the recoil lobe or an indication that the recoil lobe is of the same size as at 6.0 eV, but has rotated towards  $180^\circ$ . The center of the recoil peak appears to be close to the recoil direction.

To summarize, the binary electrons that come from events, which ionize the outer  $1\pi_g$  and leave the re-

sidual  $O_2^+$  ion in the  $X^2\Pi_g$  state are directed  $90^\circ$  to the direction of the incident beam. This direction is not a function of the ejected-electron energy or the momentum-transfer direction. The binary results for the  $a^4\Pi_u$  and  $b^4\Sigma_g^+$  states are similar to what is observed in  $N_2$ . On the other hand, the recoil results are quite different from the  $N_2$  observations. Since the recoil peak is produced by ejected electrons that subsequently collided with the molecular core, it is perhaps not surprising that such a complicated process should be different in  $O_2$  and  $N_2$ .

It is interesting to consider processes that might cause the unusual distributions reported here. The following discussion is intended to stimulate further work on these problems. Since there has been no theoretical work that specifically considered these systems, any discussion of possible mechanisms must include some speculation.

The most striking feature of the TDCS for both  $N_2$  and  $O_2$  is the very large angles, far from the momentum-transfer direction, at which some of the low-energy electrons are ejected. These large ejection angles are an indication of a strong interaction between the ejected electron and the residual ion core. The ionization process must produce a temporary polarization that causes the electrons from the  $1\pi_g$  molecular orbitals in all the randomly oriented  $O_2$  molecules to be preferentially ejected  $90^\circ$  to the incident beam direc-

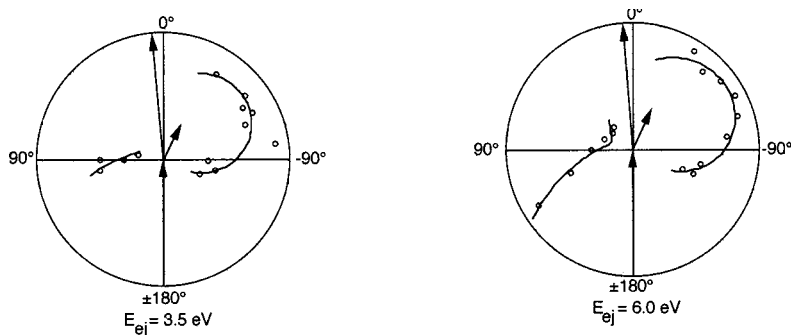


FIG. 4. Same as Fig. 2 except for ionization of the  $3\sigma_g$  orbital of  $O_2$  to give the  $b^4\Sigma_g^+$  state of the  $O_2^+$  ion. Due to the small signal at 11.0 eV, it was not possible to measure the relative TDCS at this ejected-electron energy.

tion. Kim's [14] observations on "soft" collisions, which are the same large-impact parameters, small momentum-transfer collisions we observe, may provide a clue to the process responsible. Kim points out that in these collisions, the target electron is acted on by an impulsive force that is nearly perpendicular to the direction of motion of the incident particles. In our case of  $O_2$  molecules with two unpaired electrons in an outer, antibonding orbital, this perpendicular force may be especially effective in removing an unpaired electron and sending it off  $90^\circ$  to the direction of motion of the incident electron. For the other orbitals of  $O_2$  and  $N_2$ , the long-range force exerted by the incident electron is presumably be less effective and a more direct hit on the target electron is necessary. This leads to ejection towards the momentum-transfer direction.

The ejection of binary electrons associated with ionization of the higher molecular orbitals in  $O_2$  gives distributions very similar to those observed for the analogous orbital in  $N_2$ . This occurs even though the order in energy of the orbitals is

reversed in going from  $N_2$  to  $O_2$ . This suggests that the symmetry of the orbital is more important than its position in the energy scheme.

The binary distributions for all the orbitals are quite similar. This may be a result of the comparatively small interaction of the incident electrons with all the molecular electrons in the binary ejection case. In the recoil direction, the ejected electrons presumably scatter from the molecular core. For molecules, this can obviously be a complicated process since the molecular core is not spherically symmetric. It is therefore not surprising that the recoil angular distributions are very different from the binary distributions. The origin of the very different recoil distributions for  $O_2$  compared to  $N_2$  remains an unresolved question.

#### ACKNOWLEDGMENT

This work was supported by Grant No. ATM-9705115 from the National Science Foundation.

- 
- [1] M. A. Coplan, J. H. Moore, and J. P. Doering, *Rev. Mod. Phys.* **66**, 985 (1994).
- [2] H. Ehrhardt, K. Jung, G. Knoth, and P. Schlemmer, *Z. Phys. D: At., Mol. Clusters* **1**, 3 (1986).
- [3] J. P. Doering and L. Goembel, *J. Geophys. Res.* **96**, 16 025 (1991).
- [4] J. P. Doering and J. Yang, *J. Geophys. Res.* **102**, 9683 (1997).
- [5] J. P. Doering and J. Yang, *J. Geophys. Res.* **102**, 9691 (1997).
- [6] J. P. Doering and J. Yang, *Phys. Rev. A* **60**, 2176 (1999).
- [7] J. P. Doering and J. Yang, *Phys. Rev. A* **54**, 3977 (1996).
- [8] J. Berkowitz, *Photoabsorption, Photoionization and Photoelectron Spectroscopy* (Academic, New York, 1979), p. 211.
- [9] G. Herzberg, *Spectra of Diatomic Molecules* (Nostrand, Princeton, NJ, 1950), p. 346.
- [10] J. P. Doering, J. Yang, and J. W. Cooper, *Chem. Phys. Lett.* **232**, 159 (1995).
- [11] H. Ehrhardt, K. Hesselbacher, K. Jung, E. Schubert, and K. Williams, *J. Phys. B* **7**, 69 (1974).
- [12] D. Madison and V. D. Kravtsov (private communication).
- [13] J. P. Doering and S. O. Vaughan, *J. Geophys. Res.* **91**, 3279 (1986).
- [14] Y. K. Kim, *Phys. Rev. A* **6**, 666 (1972).